

# Model of nonadiabatic-to-adiabatic dynamical quantum phase transition in photoexcited systems

Jun Chang<sup>1,2,3</sup>, Ilya Eremin<sup>4,5</sup>, Jize Zhao<sup>6,7</sup>

<sup>1</sup>College of Physics and Information Technology,  
Shaanxi Normal University, Xi'an 710119, China

<sup>2</sup>Max-Planck Institut für Physik komplexer Systeme, D-01187 Dresden, Germany

<sup>3</sup>State Key Laboratory of Theoretical Physics, Institute of Theoretical Physics, CAS, Beijing 100190, China

<sup>4</sup>Institut für Theoretische Physik III, Ruhr-Universität Bochum, D-44801 Bochum, Germany

<sup>5</sup>Kazan (Volga Region) Federal University, Kazan 420008, Russian Federation

<sup>6</sup>Institute of Applied Physics and Computational Mathematics, Beijing 100094, China

<sup>7</sup>Beijing Computational Science Research Center, Beijing 100084, China

We study the ultrafast dynamic process in photoexcited systems and find that the Franck-Condon or Landau-Zener tunneling between the photoexcited state and the ground state is abruptly blocked with increasing the state coupling from nonadiabatic to adiabatic limits. The blockage of the tunneling inhibits the photoexcited state from decaying into the thermalized state and results in an emergence of a metastable state, which represents an entanglement of electronic states with different electron-phonon coupling strengths. Applying this model to the investigation of photoexcited half-doped manganites, we show that the quantum critical transition is responsible for more than a three-orders-of-magnitude difference in the ground-state recovery times following photoirradiation. This model also explains some elusive experimental results such as photoinduced rearrangement of orbital order by the structural rather than electronic process and the structural bottleneck of a one-quarter period of the Jahn-Teller mode. We demonstrate that in the spin-boson model there exist unexplored regions not covered in the conventional phase diagram.

PACS numbers: 64.60.A-, 63.20.kd, 71.27.+a

*Introduction.*— Recent years have witnessed increasing attention to the photoinduced dynamical phase transition in strongly correlated systems. Controllable light pulses ultrafastly drive the colossal changes in optical, electronic and magnetic properties of materials, in particular, by introducing switches between various competing phases [1–12]. A photoinduced phase transition is believed to be similar to a thermally driven one because the photon energy eventually is redistributed among interacting charge, spin and lattice degrees of freedom, and hence increases the system temperature [13, 14].

However, the metastable or “hidden” phases distinct from those found in conventional phase diagrams were reported to be accessed by photoirradiation rather than thermalization in manganites [15–18], nickelates [19], organic materials [7, 20], cuprates [11] and transition metal complexes [21]. Furthermore, the study of a temporal phase is obviously out of the reach of traditional methods, where phase transitions are determined from the free energy of equilibrium states.

The lighting dynamics in manganites,  $\text{RE}_x\text{AE}_{x,2-x}\text{MnO}_{3,4}$  (RE, rare-earth ions, AE: alkaline-earth ions), is especially striking [15–18, 22]. For instance, in  $\text{Nd}_{0.5}\text{Ca}_{0.5}\text{MnO}_3$ , the excited state ultrafastly returns to the ground state within around 0.6 picoseconds (ps) after photoirradiation [23]. Surprisingly, in  $\text{Nd}_{0.5}\text{Sr}_{0.5}\text{MnO}_3$  with the same structure, a photoinduced long-lived excited state survives for about 3000 ps or 3 nanoseconds (ns) [16]. Similarly, in  $\text{La}_{0.5}\text{Sr}_{1.5}\text{MnO}_4$ , the photoexcited transient state also

lasts for ns [15]. The underlying mechanism making the enormous difference in recovery times is still not clear. Another challenge in the manganites is that the photoexcitation melts antiferromagnetic order but only partially reduces the orbital order [15]. In addition, a theoretical understanding of the structural bottleneck and photoinduced rearrangement of the orbital order by the structural rather than the electronic process [17] is timely.

In this paper, we focus on the ultrafast quantum phase transition and the formation of metastable states in the photoexcited spin-boson-like model [24]. With the aid of this model, we probe the ultrafast local electron dynamics in strongly correlated systems after low-intensity light irradiation.

*Quantum Model.*— In a strongly correlated system, optical light illumination triggers the excitation of the higher vibrational levels of phonon modes, and drives a redistribution of anisotropic  $d$  or  $f$  orbital occupations. Hence it often leads to geometric deformation or structural phase transition in the system. The locally excited state dissipates energy to its surrounding by emission of phonons or photons [25]. To elucidate this dynamical process, we introduce a model with electronic states, coupled to a phonon bath. Due to the strong electron-phonon coupling and the substantial bath memory effects in a photo-driven system, a Born-Markov master equation is insufficient to describe the ultrafast electron dynamics. For this reason, we first map the spin-boson model to an alternative model, where the electronic states

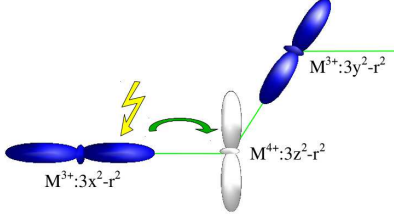


FIG. 1: (color online) Schematic photoinduced charge transfer from  $3x^2/3y^2 - r^2$  orbitals at  $\text{Mn}^{3+}$  to  $3z^2 - r^2$  and/or  $x^2 - y^2$  (not shown) orbitals at their neighboring  $\text{Mn}^{4+}$  sites in half-doped manganites. The (green) line indicates a ferromagnetic zigzag chain. Before the pump pulse,  $3z^2 - r^2$  orbitals at  $\text{Mn}^{4+}$  sites are empty. Oxygen orbitals are not shown for clarity.

with energies  $E_i$  are coupled to a single harmonic mode damped by an Ohmic bath [26]. Here, we assume that the correlations between electrons are taken into account by the effective renormalization of electronic state energies. Variations in the coupling strength  $\lambda_i$  change the equilibrium positions of different states. The system Hamiltonian is written as,

$$H_s = \sum_i E_i c_i^\dagger c_i + \sum_{ij} V_{ij} (c_i^\dagger c_j + \text{h.c.}) + \sum_i \lambda_i c_i^\dagger c_i (a^\dagger + a) + \hbar\omega a^\dagger a, \quad (1)$$

where  $c_i^\dagger c_i$  gives the occupation of the state  $i$ ,  $V_{ij}$  is the coupling (hybridization) constant that causes a transition between states  $j$  and  $i$ .  $a^\dagger$  is the creation operator for the vibrational mode with frequency  $\omega$ . We further define the energy gap  $\Delta_{ij} = (E_i - \varepsilon_i) - (E_j - \varepsilon_j)$  and electron-phonon self-energy difference  $\varepsilon_{ij} = (\lambda_i - \lambda_j)^2 / (\hbar\omega)$  between two states with  $\varepsilon_i = \lambda_i^2 / (\hbar\omega)$ . Interestingly, despite  $H_s$ 's formal similarity with the Holstein model [27], the indices  $i$  and  $j$  refer to states rather than lattice sites.

The Ohmic bath damping is introduced by a dissipative Schrödinger equation, in which a dissipative operator  $iD$  is added to the Hamiltonian to describe the bath induced state transfer,  $i\hbar\partial|\psi(t)\rangle/\partial t = (H_0 + iD)|\psi(t)\rangle$ , where  $H_0$  is the Fröhlich transformation of  $H_s$ . This equation effectively incorporates both the strong electron-phonon coupling and environment memory effects, which were described previously [28–30]. Here, we focus on the dynamics of the electronic states with electron number conservation at the low excitation photon density limit and set the temperature  $T = 0$ , as we are interested in the quantum phase transitions.

Let us specifically consider half-doped manganites as an example. The insulating ground state of this system is mostly characterized by the charge-exchange type order with the ferromagnetic (FM) zigzag chains, which couple antiferromagnetically, whereas  $\text{Mn}^{4+}$  and  $\text{Mn}^{3+}$  alternate on the chain [31–33]. An incident optical photon drives an electron transfer from the  $3x^2/3y^2 - r^2$  orbital

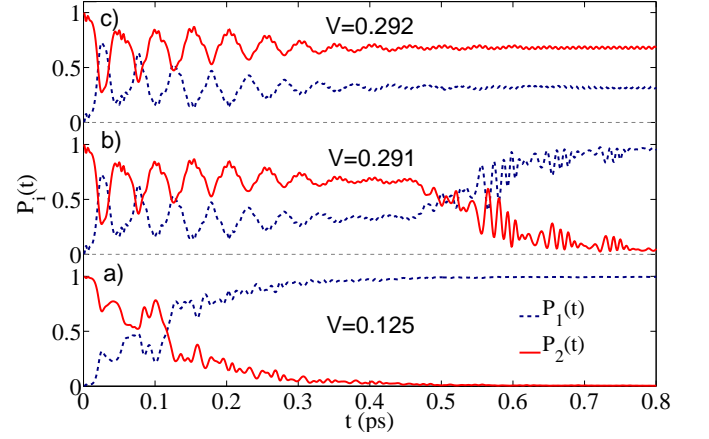


FIG. 2: (color online) The time evolution of photodriven state probabilities for  $V=0.125$  (a),  $V=0.291$  (b), and  $V = V_c=0.292$  (c). When the electronic coupling  $V$  is less than a critical value  $V_c$ , the excited state 2 returns to the ground state 1. While  $V \geq V_c$ , the relaxed state represents a strong entanglement of both the state 1 and the state 2. The slower oscillation period refers to the phonon mode of 69 fs, while the faster oscillation period of about 9–10 fs is expected from the energy gap  $\sqrt{\Delta^2 + 4V^2}$ . Here, we set  $\Delta = \varepsilon$  and  $\varepsilon = 0.4$  eV as the energy unit.

at the  $\text{Mn}^{3+}$  site to the  $3z^2 - r^2$  and/or the  $x^2 - y^2$  orbital at its neighboring  $\text{Mn}^{4+}$  site on the FM chain [17, 34]. The charge redistribution in the anisotropic  $d$  orbitals often occurs along with strong lattice oscillations. For instance, in  $\text{Nd}_{0.5}\text{Ca}_{0.5}\text{MnO}_3$ , the so-called Jahn-Teller mode is dominant to release the displacements of oxygen atoms around the Mn ions after lighting [23]. To apply the above model in the low laser intensity limit (the saturation density of excitation photons,  $0.8 \text{ mJ cm}^{-2}$ , corresponds to one photon per 60 Mn ions [16]), we label the initial state prior to the lighting as state 1, and the charge transfer state as 2. The surrounding sites are regarded as the environment. According to the optical spectra experiments [34], both the energy gap  $\Delta$  and the electron-phonon self-energy difference  $\varepsilon$  between state 1 and 2 are estimated to be around several tenths of eV. This is also in agreement with Jahn-Teller characteristic energy. We include the Jahn-Teller mode frequency  $\hbar\omega=0.06$  eV and damping time on the picoseconds time scale,  $(2\Gamma)^{-1} = 0.1$  ps following the reference [23]. It is worth noting that the decay time of a particular state is not directly related to the phonon mode damping  $\Gamma$ . As for the electronic state coupling or hybridization parameter  $V$ , its value  $((pd\sigma)^2/2)$  ranges between 0.13 and 0.33 eV in the literature [35] for the  $3x^2/3y^2 - r^2$  and  $3z^2 - r^2$  orbitals. Note, that  $pd\sigma$  is the overlap integral between the  $d\sigma$  and  $p\sigma$ -orbitals. Here, we also set  $\varepsilon = 0.4$  eV as the energy unit.

*Quantum Phase Transition.*— The first photoexcited state is set as the starting state, which keeps the same configuration coordinate as the ground state in the Born

approximation. Solving the dissipative Schrödinger equation numerically, the evolution of the photoexcited state as a function of time clearly reflects the quantum phase transition, see Fig. 2. When the hybridization is weak, i.e.  $V=0.125$ , far less than the electron-phonon coupling  $\lambda = \sqrt{\hbar\omega\varepsilon}=0.387$ , the photoexcited state relaxes to the ground state with quantum efficiency close to 100% within 0.5 ps, which is close to the recovery time 0.6 ps, found in  $\text{Nd}_{0.5}\text{Ca}_{0.5}\text{MnO}_3$ . [23] Here, we notice that our results obtained by the quantum method qualitatively agree with that of the semi-classical Franck-Condon principle [30]. Increasing  $V$  to 0.291, the photodriven state still falls back to the initial state within 1 ps (see Fig. 2 (b)). However, once  $V$  raises to the critical value  $V_c=0.292$ , the occupation probability of state 2 stays finite after around 0.5 ps. An extension of the time evolution up to 0.1 ns confirms that the long-lived excited state represents a strongly entangled mixture of states 1 and 2, which does not decay by phonon dissipation. With further increased hybridization  $V > V_c$ , the metastable state remains robust, which signals quantum phase transition to the metastable state at  $V_c$ .

*Semi-classical Model.*— Here, we present a qualitative understanding of the metastable state formation, starting from a semi-classical phenomenological model with two localized electronic states, coupled to a phonon mode with frequency  $\omega$  as shown in Fig.3. The crossing curves are parabolic nonadiabatic free-energy surfaces. The ground-states is labeled as 1 with the free-energy as a function of the configuration coordinate  $f_1 = KR^2/2 + \Delta$ , and the excited state 2 with  $f_2 = K(R - \Delta R)^2/2$ . Here,  $\Delta$  is the energy gap between two states, and their equilibrium positions are separated by  $\Delta R$ . We further define the electron-phonon self-energy  $\varepsilon = K(\Delta R)^2/2$  and the corresponding electron-phonon coupling strength  $\lambda = \sqrt{\hbar\omega\varepsilon}$ . The excited state relaxes to the original state via the weak energy splitting at the free energy surface cross point [36] according to the Franck-Condon principle or Landau-Zener tunneling in the weak-coupling limit, i.e. when the strength of the electronic state coupling  $V \ll \lambda$ .

The solid anti-crossing curves of adiabatic free energy surfaces are described by  $\epsilon_{\pm} = (f_1 + f_2 \pm \sqrt{(f_1 - f_2)^2 + 4V^2})/2$ . The energy gap near the avoided crossing is about  $2V$ . The photoexcited state relaxes to the bottom of the upper potential energy curve as shown in Fig. 3, whereas the thermally excited state stays on the lower energy curve in the adiabatic limit  $V \gg \lambda$ .

This classical model has been extensively used to explain many experimental results. For example, Marcus' theory adopts this model to give the probability of interconversion of donor and acceptor through the region near the intersection of potential energy surfaces in the non-adiabatic limit [37]. However, the metastable state

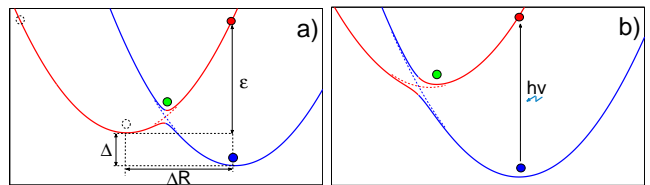


FIG. 3: (color online) Schematic free energy as a function of the configuration coordinate for two energy levels, coupled to the harmonic phonon mode. The parabolic curves are nonadiabatic free energy surfaces in the weak-coupling limit. The electronic coupling caused splitting at the cross point is neglected. The photoexcited state reaches the ground state by Franck-Condon or Landau-Zener tunneling. The solid anti-crossing curves refer to the adiabatic free energy surfaces, and the energy gap (about  $2V$ ) at the avoided crossing point blocks the tunneling and separates the photoexcited states from the thermalized states on the lower potential energy curve. Consequently, the photoinduced states (red dots) relax to the bottom of the higher curves (green dots with energy  $E_c$ ). Here,  $\Delta$  and  $\varepsilon$  are the energy gap and electron-phonon self-energy difference between the two levels, respectively.

often refers to the thermally induced state in the bottom of the lower adiabatic free energy surfaces [37, 38], represented by the lower dashed circle in Fig. 3(a). As clearly seen it is distinctly different from our proposed photoinduced metastable state in the bottom of the upper anti-crossing curves (green dots). Particularly, there is no classical metastable state when  $\Delta$  is close to  $\varepsilon$  (see Fig. 3(b)). Additionally, the nonequilibrium phase transition is also out of reach of the semi-classic model. We have shown that a solution of the time dependent Schrödinger equation provides a practical approach to study the dynamical phase transition process, not restricted to the adiabatic or nonadiabatic limits.

*Metastable State.*—To verify the robustness of the metastable state, we vary the energy gap away from the electron-phonon self-energy. We find that the photoinduced quantum metastable state still exists and its state energy  $E_q$  is quite close to the classical free energy  $E_c$ , shown at the bottom of the upper adiabatic curves in Fig. 3 (green circles). The inset of Fig.4 shows the critical strength of the state coupling  $V_c$  for the formation of the metastable states. However, we find that  $E_q$  is also close to the energy gap  $\Delta$ , which is often referred to as the classical metastable state energy, see Fig. 4. To further confirm our phenomenological picture for the metastable state, we prepare some thermalized initial states and study their time evolution in the dissipative Schrödinger equation. For example, turning the coupling between the states off, we put the starting state to those, indicated by the dashed circles in Fig.3, and then turn the electric coupling on. Regardless of the coupling being larger or lesser than the critical  $V_c$ , these thermalized states decay to the ground state within 1 ps without long-

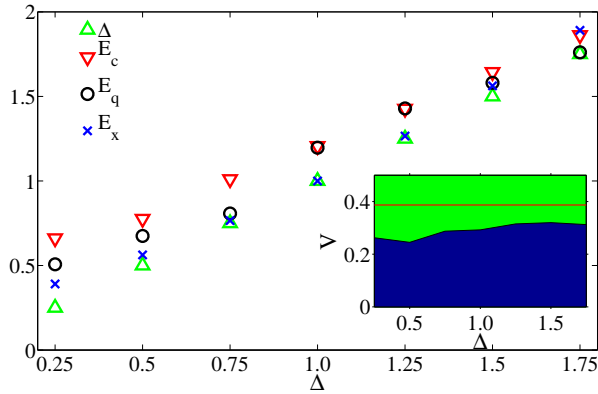


FIG. 4: (color online) The photoinduced metastable state phase diagram. The energies of the photoinduced quantum metastable state  $E_q$  are located below the energies  $E_c$  at the bottom of the upper adiabatic curves, shown in Fig. 3, and above the energy gap  $\Delta$ .  $E_x$  is the free energy at the cross point of the nonadiabatic curves. The inset shows critical strength of the state coupling  $V_c$  for the formation of the metastable state. The (red) straight line indicates the electron-phonon coupling  $\lambda$ .

lived metastable states, at least in the parameter space of this paper. This also suggests the impossibility for thermalization to excite the ‘hidden’ phases in experiments.

*Discussion and Conclusion.*— Our results for the dynamical phase transition allow us to clarify some elusive experimental results, for instance, the three order of magnitude difference in the ground state recovery times between  $\text{Nd}_{0.5}\text{Sr}_{0.5}\text{MnO}_3$ ,  $\text{La}_{0.5}\text{Sr}_{1.5}\text{MnO}_4$  and  $\text{Nd}_{0.5}\text{Ca}_{0.5}\text{MnO}_3$ . We believe that the photoexcited state falls back to the ground state within 1 ps in  $\text{Nd}_{0.5}\text{Ca}_{0.5}\text{MnO}_3$  without formation of the metastable state, which could be due to the hybridization  $V$  being less than the critical value  $V_c$  [23]. At the same time, the photoinduced excited state relaxes to the transient state in the other two compounds [15, 16], as the long-lived excited state does not decay by the phonon, and alternatively, it relaxes to the initial state by the spontaneous emission of fluorescence photons with a characteristic relaxation time of 1~100 ns. As for the antiferromagnetic order destroyed in layer manganites  $\text{La}_{0.5}\text{Sr}_{1.5}\text{MnO}_4$ , we propose here that the charge transfer occupation of the  $3z^2-r^2$  orbitals increases the layer spacing and further reduces the already weak layer antiferromagnetic coupling, and AF order is consequently suppressed [15]. On the other hand, orbital order is only partially reduced because a recurrence to the initial state occurs after the charge transfer from  $3x^2/3y^2-r^2$  to  $3z^2-r^2$  within tens of fs as shown in Fig 2(c). Meanwhile, a drop time, about a one-quarter period of the Jahn-Teller mode, is obtained by the error function fit of the charge transfer state probability evolution with time in the Fig 2(c). This is in agreement with the experiment, which observes 18 fs bottleneck for the loss of the orbital order [17]. The

transient metastable state is then a strong entanglement of the Jahn-Teller orbital doublet, which is also consistent with the experimental evidence of photoinduced rearrangements of orbital order by the structural rather than the electronic process in a recent birefringence experiment [17].

To summarize, we have solved the dissipative Schrödinger equation for a two level system in phonon bath to simulate the ultrafast time evolution of local quantum states in photoexcited strongly correlated systems. A dynamical quantum phase transition is indicated by the formation of a metastable state with increasing the state coupling from nonadiabatic to adiabatic limits. By the semi-classical model, we show that the emergent transient metastable states could be stabilized by the blockage of the Landau-Zener tunneling near the avoided crossing, distinctly different from the conventional stabilization of transient charge or orbital order by the on-site or inter-site Coulomb repulsion. This vibronic mechanism is substantiated by the recent optical birefringence experiment [17]. The dynamics from nonadiabatic to adiabatic limit experiences a quantum phase transition rather than a gradual process. This physical picture also could be extended towards understanding the photoinduced formation of temporal hidden phases in other transition metal or rare earth systems [19], organic materials [7, 20], transition metal complexes [21] and potentially even the systems with Dirac cones. We further expect that the pressure induced change of electronic states coupling may potentially drive the quantum phase transition in a single material, e.g.  $\text{Nd}_{0.5}\text{Ca}_{0.5}\text{MnO}_3$ . Our work demonstrates that there exist hidden regions in conventional phase diagrams when correlated systems are driven out of equilibrium.

*Acknowledgments.*—We are thankful to Yang Ding, Javier Fernandez Rodriguez, Michel van Veenendaal, Stefan Kirchner, Peter Thalmeier, Roderich Moessner and Shaojin Qin for fruitful discussions. J.C is supported by the Fundamental Research Funds for the Central Universities, GK201402011, and SNNU’s seed funds. The work of I.E. is supported by the Mercator Research Center Ruhr (MERCUR) and the Russian Government Program of Competitive Growth of Kazan Federal University. J.Z. is supported by NSFC 11474029.

- 
- [1] K. Miyano, T. Tanaka, Y. Tomioka, and Y. Tokura, Phys. Rev. Lett. **78**, 4257 (1997).
  - [2] S. Koshihara, Y. Tokura, T. Mitani, G. Saito, and T. Koda, Phys. Rev. B **42**, 6853 (1990).
  - [3] K. Nasu, Photoinduced Phase Transitions (World Scientific, 2004).
  - [4] M. Rini, R. Tobey, N. Dean, J. Itatani, Y. Tomioka, Y. Tokura, R. W. Schoenlein, and A. Cavalleri, Nature (London) **449**, 72 (2007).

- [5] A. Caviezel, U. Staub, S. L. Johnson, S. O. Mariager, E. Möhr-Vorobeve, G. Ingold, C. J. Milne, M. Garganourakis, V. Scagnoli, S. W. Huang, et al., *Phys. Rev. B* **86**, 174105 (2012).
- [6] T. Li, A. Patz, L. Mouchliadis, J. Yan, T. A. Lograsso, I. E. Perakis, and J. Wang, *Nature (London)* **496**, 69 (2013).
- [7] M. Hoshino, S. Nozawa, T. Sato, A. Tomita, S.-i. Adachi, and S.-y. Koshihara, *RSC Adv.* **3**, 16313 (2013).
- [8] Y. Chuang, W. Lee, Y. Kung, A. Sorini, B. Moritz, R. Moore, L. Patthey, M. Trigo, D. Lu, P. Kirchmann, et al., *Phys. Rev. Lett.* **110**, 127404 (2013).
- [9] P. Beaud, S. L. Johnson, E. Vorobeve, U. Staub, R. A. D. Souza, C. J. Milne, Q. X. Jia, and G. Ingold, *Phys. Rev. Lett.* **103**, 155702 (2009).
- [10] M. Först, R. I. Tobey, S. Wall, H. Bromberger, V. Khanna, A. L. Cavalieri, Y.-D. Chuang, W. S. Lee, R. Moore, W. F. Schlotter, et al., *Phys. Rev. B* **84**, 241104 (2011).
- [11] D. Fausti, R. Tobey, N. Dean, S. Kaiser, A. Dienst, M. Homann, S. Pyon, T. Takayama, H. Takagi, and A. Cavalleri, *Science* **331**, 189 (2011).
- [12] S. Wall, D. Prabhakaran, A. T. Boothroyd, and A. Cavalleri, *Phys. Rev. Lett.* **103**, 097402 (2009).
- [13] S. I. Anisimov, B. L. Kapeliovich, and T. L. Perel'man, *Zh. Eksp. Teor. Fiz.* **66**, 776 (1974), [*Sov. Phys. JETP* **39**, 375 (1974)].
- [14] E. Beaurepaire, J.-C. Merle, A. Daunois, and J.-Y. Bigot, *Phys. Rev. Lett.* **76**, 4250 (1996).
- [15] H. Ehrke, R. I. Tobey, S. Wall, S. A. Cavill, M. Först, V. Khanna, T. Garl, N. Stojanovic, D. Prabhakaran, A. T. Boothroyd, et al., *Phys. Rev. Lett.* **106**, 217401 (2011).
- [16] H. Ichikawa, S. Nozawa, T. Sato, A. Tomita, K. Ichiyanaagi, M. Chollet, L. Guerin, N. Dean, A. Cavalleri, S.-i. Adachi, et al., *Nat. Mater.* **10**, 101 (2011).
- [17] R. Singla, A. Simoncig, M. Forst, D. Prabhakaran, A. L. Cavalieri, and A. Cavalleri, *Phys. Rev. B* **88**, 075107 (2013).
- [18] R. I. Tobey, S. Wall, M. Först, H. Bromberger, V. Khanna, J. J. Turner, W. Schlotter, M. Trigo, O. Krupin, W. S. Lee, et al., *Phys. Rev. B* **86**, 064425 (2012).
- [19] W.-S. Lee, Y. Chuang, R. Moore, Y. Zhu, L. Patthey, M. Trigo, D. Lu, P. Kirchmann, O. Krupin, M. Yi, et al., *Nat. Commun.* **3**, 838 (2012).
- [20] K. Onda, S. Ogihara, K. Yonemitsu, N. Maeshima, T. Ishikawa, Y. Okimoto, X. Shao, Y. Nakano, H. Yamochi, G. Saito, et al., *Phys. Rev. Lett.* **101**, 067403 (2008).
- [21] T. Tayagaki and K. Tanaka, *Phys. Rev. Lett.* **86**, 2886 (2001).
- [22] T. Ogasawara, T. Kimura, T. Ishikawa, M. Kuwata-Gonokami, and Y. Tokura, *Phys. Rev. B* **63**, 113105 (2001).
- [23] H. Matsuzaki, H. Uemura, M. Matsubara, T. Kimura, Y. Tokura, and H. Okamoto, *Phys. Rev. B* **79**, 235131 (2009).
- [24] A. J. Leggett, S. Chakravarty, A. T. Dorsey, M. P. A. Fisher, A. Garg, and W. Zwerger, *Rev. Mod. Phys.* **59**, 1 (1987).
- [25] U. Weiss, *Quantum Dissipative Systems* (World Scientific, Singapore, 2000).
- [26] A. Garg, J. Onuchic, and V. Ambegaokar, *J. Chem. Phys.* **83**, 4491 (1985).
- [27] T. Holstein, *Ann. Phys.* **8**, 325 (1959).
- [28] J. Chang, A. J. Fedro, and M. van Veenendaal, *Chem. Phys.* **407**, 65 (2012).
- [29] M. van Veenendaal, J. Chang, and A. J. Fedro, *Phys. Rev. Lett.* **104**, 067401 (2010).
- [30] J. Chang, A. J. Fedro, and M. van Veenendaal, *Phys. Rev. B* **82**, 075124 (2010).
- [31] Z. Jiráček, S. Krupička, Z. Šimša, M. Dlouhá, and S. Vratislav, *J. Magn. Magn. Mater.* **53**, 153 (1985), ISSN 0304-8853.
- [32] B. J. Sternlieb, J. P. Hill, U. C. Wildgruber, G. M. Luke, B. Nachumi, Y. Moritomo, and Y. Tokura, *Phys. Rev. Lett.* **76**, 2169 (1996).
- [33] Y. Murakami, H. Kawada, H. Kawata, M. Tanaka, T. Arima, Y. Moritomo, and Y. Tokura, *Phys. Rev. Lett.* **80**, 1932 (1998).
- [34] Y. Okimoto, Y. Tomioka, Y. Onose, Y. Otsuka, and Y. Tokura, *Phys. Rev. B* **59**, 7401 (1999).
- [35] E. Dagotto, T. Hotta, and A. Moreo, *Phys. Rep.* **344**, 1 (2001).
- [36] D. R. Yarkony, *Rev. Mod. Phys.* **68**, 985 (1996).
- [37] R. A. Marcus, *Rev. Mod. Phys.* **65**, 599 (1993).
- [38] W. A. Tisdale and X.-Y. Zhu, *PNAS* **108**, 965 (2011).